16th World Conference on Earthquake, 16WCEE 2017
Santiago Chile, January 9th to 13th 2017
Paper N° 4164
Registration Code: S-T1464750342

MULTI-HAZARD ASSESSMENT OF STEEL BUILDINGS RETROFITTED USING PASSIVE CONTROL DEVICES

T. Roy[(1)], V.A. Matsagar[(2)]

[(1)] Ph.D. Research Scholar, Indian Institute of Technology (IIT) Delhi, Hauz Khas, Delhi, India. tathagata.roy@civil.iitd.ac.in
[(2)] Associate Professor, Indian Institute of Technology (IIT) Delhi, Hauz Khas, Delhi, India. matsagar@civil.iitd.ac.in

Abstract

The multi-hazard effects on multi-story steel buildings retrofitted either by bracing systems or energy dissipating passive vibration control devices is assessed for its performance under earthquake- and wind-induced forces. The passive vibration control devices used in this investigation include steel bracing, viscous, and viscoelastic dampers. The buildings without and with the passive control devices are modeled as multi-degree of freedom (M-DOF) systems, with the seismic masses lumped at each floor level. The governing differential equations of motion for the uncontrolled and controlled buildings are solved by using Newmark's time integration approach. The dynamic response quantities are compared, which include the floor acceleration, inter-storey drift, column base shear, and floor displacement, for the existing and retrofitted buildings subjected to earthquake- and wind-induced forces independently. Joint probabilities of failure are determined in terms of probability density function (PDF) and cumulative distribution function (CDF) by conducting fragility analysis to assess the effectiveness of the retrofit scheme against each natural hazard. It is concluded that upon retrofitting the buildings using the passive control devices, the forces attracted during the two hazards depend mainly on their modified dynamic properties, such as modal frequencies and added damping, which in turn affects the response reduction achieved. It is evident that under the wind loads the control systems which are effective in reducing the forces, limiting the large displacement, under the earthquake loads, tend to attract increased forces. Conversely, a flexible system effective in the seismic response control may prove to be ineffective for the wind response control. Thus, a retrofit strategy providing beneficial effects against a hazard may prove to be detrimental for the other, which calls upon careful selection of the retrofit solution and design for a structure considering such multi-hazard scenario.

Keywords: Earthquake; Fragility; Joint probability; Multi-hazard; Retrofit; Steel building; Wind

1. Introduction

Careful attention towards the devastations caused due to multi-hazard effects emerged at the beginning of the 21st century, when risks against multiple natural hazards posed significant threat to the modern civil infrastructure. The consequences of these multi-hazard events include: fatalities, building damages, destructions to the strategically important lifeline structures, critical service failures, and socio-economic losses. Events, such as, earthquake and gusty wind are indeed capable of huge devastation, leading to severe socio-economic losses. Multi-hazard risk assessment involves significant challenges due to the contradictory features of the processes involved in the devastation. For mid- to high-rise buildings and important structures, such as, elevated liquid storage tanks, cable-stayed bridges, the extreme threats posed to the structural members are due to earthquakes and strong winds. The nature of the loads imparted by the earthquakes and strong winds is completely different from each other, one dominated by high frequency and the other, by low frequency. The structural design differs widely for both the hazards as earthquake favors higher ductility and wind favors higher stiffness.

Earlier studies [1] on the structural risk assessment were based on a combination of loads in a given time, which lead to conservative designs. Ellingwood et al. [2] developed a fragility analysis method for evaluating the response of light-frame wood construction exposed to severe windstorms and earthquakes, useful to improve building code for loss and insurance assessments. The methodology proposed therein had the potential to provide effective strategy for improving the performance and structural safety to mitigate socio-economic losses from the threats imposed by the natural hazards. Duthinh and Simiu [3] presented a multi-hazard approach to modify the American Society of Civil Engineers' Standard, ASCE-7-2005 for safety of structures in strong wind and earthquake-prone regions. The provisions penned in the code concerning the structural design are uncertain about the intimidating effects of the multi-hazard [3]. The conclusions were drawn that hypothetical risk of exceedance of limit states prescribed in the ASCE-7-2005 may increase two-folds on considering the significant wind and earthquake hazards. Kameshwar and Padgett [4] adopted parameterized fragility-based multi-hazard risk assessment (PF-MHRA) procedure to assess the risk posed to highway bridges under the combination of earthquake and hurricane loads. The outcomes served a useful tool for rapid initial post-disaster assessment of the existing bridges to assess their risk and vulnerability, necessary to retrofit under the multiple hazards. Gehl and D'Ayala [5] proposed an approach to derive multi-hazard fragility functions using system reliability methods and Bayesian networks. Multi-hazard assessment is gaining attention in the design and retrofit of structures primarily to identify the mitigation options against catastrophe. However, it may be observed that a remedial and counteractive measure for one hazard may worsen the response of the structure due to another hazard [6]. Fur et al. [7] presented a procedure to design a second-order dynamic controller with collocated sensors for vibration control of tall buildings under seismic and wind loads. Chandrasekaran and Banerjee [8] studied optimization of retrofit design for bridges to enhance the performance and resiliency under multi-hazard effects due to the earthquake and flood-induced scours. The procedure yielded optimized retrofit design solutions by maximizing resilience and minimizing retrofit cost. The concept of the multi-hazard structural assessment is attracting attention of the structural designers, code writers, and policy-makers to amend the standard code provisions judiciously in making hazard resilient society for the days to come by.

To address the above-mentioned gap, which relates to the retrofit for one hazard and its consequent effects on the structural response under another hazard, the present work is undertaken. Herein, a multi-hazard assessment of mid- to high-rise steel buildings retrofitted with various passive control devices, such as, steel bracing (SB), fluid viscous damper (FVD), and viscoelastic damper (VED) is conducted. The specific objectives of the present investigation are: (i) to study the response of the moment resisting frame (MRF) and the retrofitted buildings under a set of stochastic earthquake and wind loads; (ii) to assess the joint probability of failure for the chosen performance level of the limit states of failure for the MRF and the retrofitted buildings in terms of probability density functions (PDFs); and (iii) to carry out fragility analyses by obtaining the failure probability of the structures in terms of cumulative distribution functions (CDFs) for earthquake and wind hazards.

2. Theory of Multi-Hazard Assessment and Joint Probability

The combination of probabilistic definitions for the hazards and vulnerabilities results in determination of structural safety on probabilistic scale. Extensive research is already conducted to define and calculate the limit states of failure of buildings to estimate the vulnerability under a particular hazard. However, in case of the structures exposed to multi-hazard scenario, the concept of joint probability is applied by the convolution theory. Fig. 1 shows fast Fourier transform (FFT) amplitudes for typical earthquake and wind excitations. Multi-hazard scenario for structural assessment arises when the modal frequencies of structures lie within the overlapped frequency band (Fig. 1). The following theory demonstrates the joint probability used for the multi-hazard scenario under the earthquake and wind hazards.

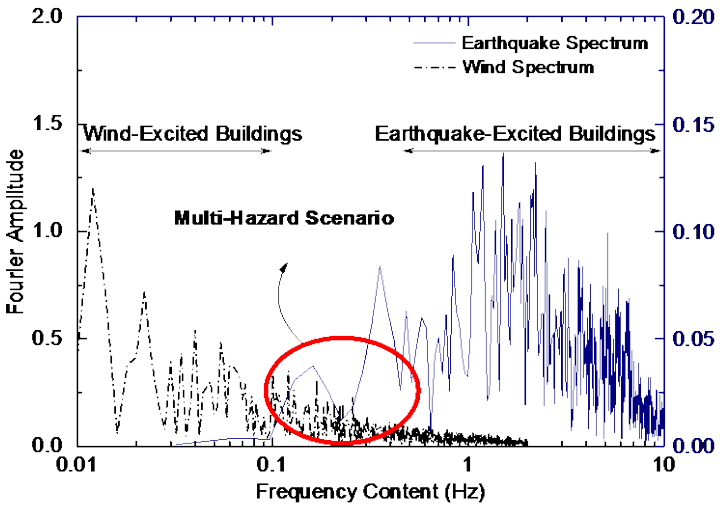

Fig. 1 - Comparison of FFT amplitude spectrum for a typical earthquake and wind time-history load

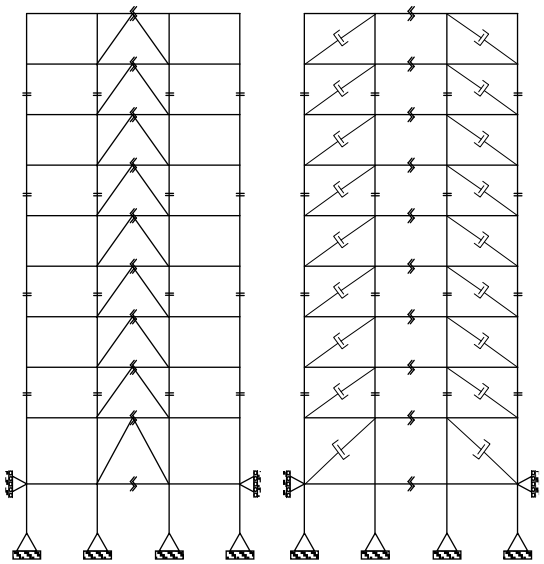

Fig. 2 - Configuration of steel bracing (left) and damper (right) in 9-storey building

Let E and W be the random variables associated with the occurrence of earthquake and wind. $P(E) = e$ is the probability of event E (earthquake) occurring, and $P(W) = w$ is the probability of event W (wind) occurring. Joint probability distribution function is defined to relate both the random variables, E and W, and for two sets of positive real numbers X and Y, such as,

$$P(E \in X, W \in Y) = P(E \in X)P(W \in Y) \tag{1}$$

In other words, the events corresponding to the multi-hazard scenario, E and W are independent for all positive real numbers a and b, the consequent events $E_A = E \in X$ and $W_B = W \in Y$ are similarly independent. Hence, for all positive real numbers,

$$P(E_A \le a, W_B \le b) = P(E_A \le a)P(W_B \le b) \tag{2}$$

Since, E and W are discrete random variables, the condition of independence in Eq. 1 corresponding to all sets of positive real numbers (a, b) becomes,

$$p(a,b) = p_E(a)\,p_W(b) \tag{3}$$

where, $p_E = P(E)$ and $p_W = P(W)$ are the probability mass functions associated with the multi-hazard events (earthquake and wind). This can be modified in the form of conditional probability as,

$$p = \sum_{e=0}^{\infty}\sum_{w=0}^{\infty} p_E(E = e \cap W = w)p_W(W = w \cap E = e) \tag{4}$$

For the independent events E and W, the joint probability distribution function F for all a and b is given by,

$$F(a,b) = F_{\mathrm{E}}(a)F_{\mathrm{W}}(b) \tag{5}$$

where, $F_{\mathrm{E}}(\cdot)$ and $F_{\mathrm{W}}(\cdot)$ are the probability density functions of earthquake and wind occurrences, respectively.

If the capacity *C* of structural members is less than the demand *D* posed due to two mutually exclusive hazards, earthquake and wind loads, then Eq. 4 can be modified for failure probability as,

$$p_{\mathrm{f}} = \sum_{e=0}^{\infty}\sum_{w=0}^{\infty} p(C < D \mid E,W)\,p_{\mathrm{E}}(E = e_{\mathrm{L}})\,p_{\mathrm{W}}(W = w_{\mathrm{L}}) \tag{6}$$

where, $p_{\mathrm{E}}(E = e_{\mathrm{L}})$ and $p_{\mathrm{W}}(W = w_{\mathrm{L}})$ are marginal mass functions of the events, *E* and *W*, respectively. If *LS* is the condition for limit state that capacity *C* be less than the demand *D* due to both the hazards *E* and *W* $p_{\mathrm{E}}\left[LS \mid (E = e_{\mathrm{L}} \cap W = w_{\mathrm{L}})\right]$ and $p_{\mathrm{W}}\left[LS \mid (W = w_{\mathrm{L}} \cap E = e_{\mathrm{L}})\right]$ are the probabilities that the limit state (*LS*) is reached at assumed loads e_{L} and w_{L} (due to the multi-hazard, *E* and *W*), truncated as $p_{\mathrm{E}}(LS \mid E,W)$ and $p_{\mathrm{W}}(LS \mid W,E)$, respectively. However, as the hazard events are mutually exclusive and collectively exhaustive, Eq. 6 can be expressed in terms of continuous random variables given as,

$$p_{\mathrm{f}} = \int_{e=0}^{\infty}\int_{w=0}^{\infty} F_{\mathrm{r}}(e,w)\,g_{\mathrm{E}}(e)\,g_{\mathrm{W}}(w)\,dw\,de \tag{7}$$

where, $F_{\mathrm{r}} = \Phi[(1/\beta)\log(x/\bar{x})]$ is the fragility expressed as joint cumulative distribution function in terms of the multi-hazard demands *E* and *W*; Φ is the normal cumulative distribution function; β is the variability associated with the demands; and $\bar{x}$ is the median value of the demand, x. The joint hazard functions are represented by $g_{\mathrm{E}}(e)$ and $g_{\mathrm{W}}(w)$ for the mutually exclusive multi-hazard events, *E* and *W*.

3. Modeling of the Retrofitted Building with the Passive Control Devices

A multi-hazard assessment is conducted on mid- to high-rise steel buildings installed with the passive control devices, such as, steel bracing (SB), fluid viscous damper (FVD), and viscoelastic damper (VED). The plane frame models of the 9-storey and 20-storey benchmark steel buildings are developed using prismatic beam element with two nodes (Fig. 2) [9, 10]. Each node has two translational- (longitudinal and transverse) and a rotational- degree-of-freedom (DOF). The geometric properties, such as, length, area, and moment of inertia and material properties, such as, mass density, Poisson's ratio, and modulus of elasticity are taken from the literature [9, 10]. The global consistent mass and stiffness matrices are determined as functions of the properties of the elements. The assemblage of the global mass and stiffness matrices from the elemental mass and stiffness matrices is carried out by summing the mass and stiffness linked with each element DOF for the entire structure.

Extensive research has been conducted on the mathematical modeling of the chosen retrofit devices. Concentric-brace (CB) provide an effective retrofit system to achieve desired higher lateral stiffness and strength required in seismic resistant design. Such metallic steel dampers also absorb energy through hysteretic cycles in a vibrating system. The global behavior of such structural system is governed by the brace in both the elastic and plastic ranges. The design parameters of such an assemblage include the yield displacement and stiffness of the brace in some proportion, κ of the storey stiffness. However, in the present study, the concentric steel bracing is modeled by making the following assumptions: (i) the steel bracing is not allowed to yield in tension and buckle in compression (no in-elastic damping), and (ii) out-of-plane failure of the metallic brace is neglected and only the in-plane stiffness is incorporated. The CB is modeled as truss elements to transfer the lateral seismic or wind loads in the form of compression or tension in the axial direction. The principle of fluid viscous damper is based on the force output proportional to the fractional power law of velocity, which corresponds to the linear Newtonian model [11]. In the present work, the non-linear fluid viscous damper (FVD) using damping coefficient method is modeled with the non-linear exponent, α. The viscoelastic damper (VED) is modeled by modal strain energy method to predict the equivalent structural damping. The steel buildings with these dampers are treated as dual systems with the moment resisting frame (MRF) as primary system, exhibiting linear behavior and the non-linear energy dissipating devices as bracing system, exhibiting elasto-plastic behavior. Hence, these

energy-dissipating devices are chosen appropriately to study their effectiveness when used in the mid- to high-rise buildings under the multi-hazard scenario.

In addition to the 9- and 20-storey buildings, a 25-storey building is designed for the gravity loads by extending the stories of the 20-storey benchmark steel building, and checked against the limit states of collapse and serviceability. Fig. 2 shows the elevation of the 9-storey steel building, showing the arrangement of the passive control devices; note that, the configurations are similarly chosen for the 20- and 25-storey buildings. The buildings without and with the passive control devices are modeled as multi-degree freedom of freedom (M-DOF) systems, with masses lumped at each floor level. The governing differential equations of motion for the uncontrolled and controlled buildings are derived and free vibration analysis is conducted to determine modal frequencies. Further, the equations are solved using Newmark's time integration approach, with linear acceleration, for the uncontrolled and controlled buildings.

4. Stochasticity of the Hazards

4.1 Earthquake hazard

The seismic hazard follows probabilistic distribution of spectral acceleration, duration of excitation, frequency content, magnitude of earthquake, epicenter distance, etc. [12]. Ground motions play an important role in assessing the dynamic response of structures, and hence, a large number of ground motions are taken for this simulation. The ground motions are represented by stochastic parameters, in terms of mean, μ_e and standard deviation, σ_e while simulating the responses of the buildings. Lognormal distribution type is assumed to study the stochasticity of the set of ground motions. For realistic results in this analysis, the ground motions are scaled with respect to the peak ground acceleration (PGA), which is considered the earthquake hazard parameter here.

4.2 Wind hazard

The stochastic wind hazard at a location is expressed as a probability density function (PDF) of the maximum wind speed for the site. The distribution function follows generalized extreme value (GEV) distribution to predict the design wind speed (Gumbel-type distribution). Mean speed of the wind profile varies with the height above the ground (z), air density (ρ_A), etc. However, in many design codes and building standards of wind loading, a peak gust speed, $U_{3s\text{-}10}$ (3-second gust speed at 10 m height from the ground), is used to calculate the design wind loads. The wind loads, with static and fluctuating components, are simulated from NatHaz online wind simulator (NOWS): simulation of Gaussian multivariate wind fields [13]. The simulation technique involves obtaining discrete frequency function with Cholesky decomposition and fast Fourier transform (FFT) for wind speed, which is considered as the wind hazard parameter here. The time histories of the wind speeds are obtained thence by summing the static and the fluctuating components obtained from the simulation based on Bernoulli's theorem.

5. Numerical Study

Multi-hazard assessment of the 9-, 20-, and 25-storey steel buildings retrofitted with the passive control devices under earthquake and wind hazard is studied. Retrofitting of the steel buildings is carried out by adding either stiffness and/or damping. In this study, the proportional stiffness for the passive control devices assumed is κ = 60% of the storey stiffness and the proportional damping assumed is ξ = 15% of the critical damping. The numerical study is conducted in two distinct protocols, deterministic and probabilistic, to investigate the effectiveness of the retrofitting systems under the multi-hazard scenario.

5.1 Deterministic analysis

Deterministic analysis involves obtaining the time domain response in terms of top floor displacement of the steel buildings under the wind and earthquake loads. Two historical earthquakes, viz., (i) the N-S component of the Imperial Valley earthquake recorded at the Imperial Valley Irrigation District substation in El Centro, California on May 18th, 1940, and (ii) the N-S component of the Northridge earthquake recorded at the Sylmar County Hospital parking lot in Sylmar, California on January 17th, 1994. Wind time history analysis is similarly

conducted for the steel buildings under the dynamic loads induced due to the basic wind speeds of 47 m/s and 55 m/s with cutoff frequency 0.3 Hz and exposure category B defined in the ASCE-7-2005. From Fig. 3 through Fig. 4, it is observed that the added stiffness increases the modal frequencies of the buildings retrofitted by the steel bracing and viscoelastic damper under the earthquakes; however, the displacement response of the retrofitted buildings increases marginally due to nature of response spectra for these frequencies. Added damping significantly reduces the displacement response of the buildings retrofitted using the fluid viscous damper under the earthquakes. From Fig. 5 through Fig. 6, it is observed that on addition of the stiffness significant displacement response reduction is achieved against the wind. Similarly, it is observed that the effect of damping is negligible on the displacement response of the steel buildings retrofitted using the fluid viscous damper under the wind. Hence, it is concluded that addition of either stiffness or damping may show improved effectiveness against a particular hazard, on the contrary, possible ineffectiveness against the other hazard.

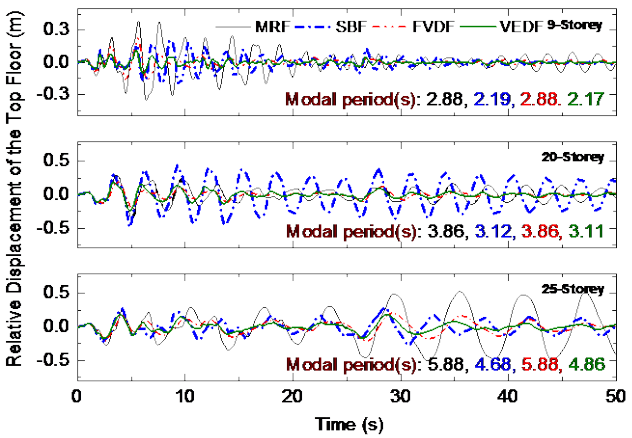

Fig. 3 - Top floor displacement time history of the steel buildings under Imperial Valley, 1940 earthquake

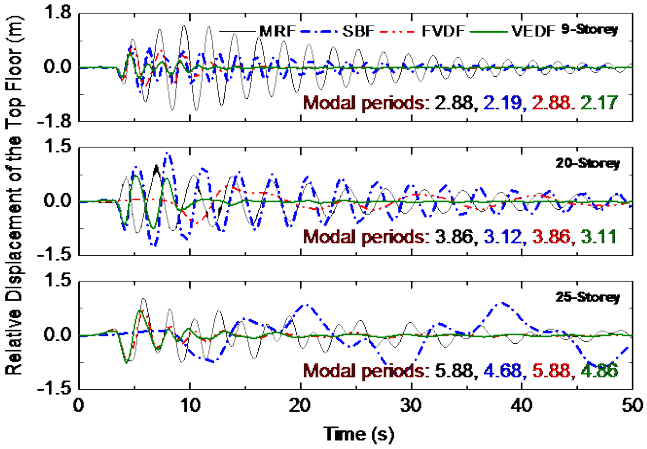

Fig. 4 - Top floor displacement time history of the steel buildings under Northridge, 1994 earthquake

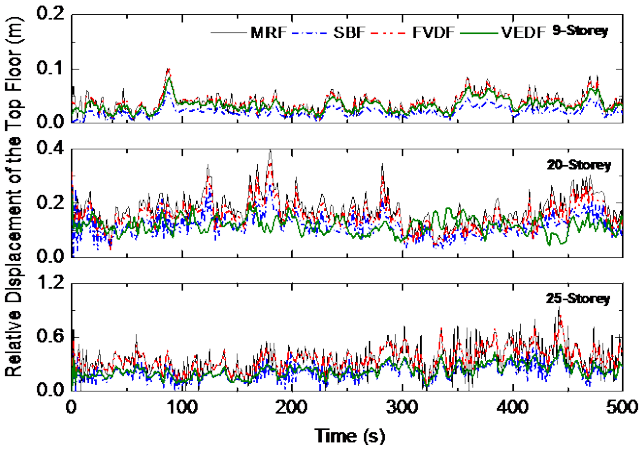

Fig. 5 - Top floor displacement time history of the steel buildings under basic wind speed, 47 m/s

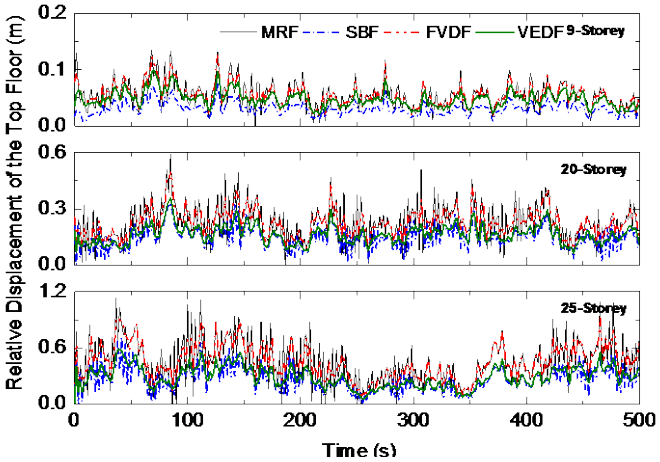

Fig. 6 - Top floor displacement time history of the steel buildings under basic wind speed, 55 m/s

5.2 Probabilistic analysis

Herein, probabilistic analysis is conducted for the 9-, 20-, and 25-storey moment resisting steel buildings retrofitted with the passive control devices under a set of earthquake and wind loads. Table 1 presents the stochastic parameters of 50 real-time earthquakes [14] and 200 simulated wind data used in the analysis of the buildings. The ground motion records are scaled up to 1*g* with respect to the PGA (*g* denotes gravitational acceleration). Limit states, such as, top floor acceleration, inter-storey drift, base shear, and top floor displacement are chosen to find out the probability of exceedance for the steel buildings. A performance level of 'extensive damage' is assumed for the limit states, with the respective limits of 2 m/s^2, 1%, 0.1*W*, and 1%, where, *W* is total weight of the building [15]. The joint probability of failure is obtained from the overlapped

area of the failure probability density functions (PDFs) for the steel buildings retrofitted with the passive control devices under the earthquake and wind hazards. The peak response quantities follow lognormal distribution of the PDF. Fragility curves, in terms of cumulative distribution functions (CDFs), are obtained to determine the probability of failure for the steel buildings retrofitted by the passive control devices under the multi-hazard scenario. Thereafter, the effectiveness of the retrofit strategy for the multi-hazard scenario in terms of joint probability from the PDFs and probability of failure from the fragility curves are studied.

Table 1 - Statistics of the stochastically generated parameters of the earthquake and wind excitations.

Case	Distribution Type	Mean	Standard Deviation	Median	Skewness	Kurtosis
Earthquake	Lognormal	μ_e = -1.12g	σ_e = 0.62g	0.32g	1.77	3.87
Wind	Extreme Value (EV)	μ_w = 47 m/s	σ_w = 5.6 m/s	43.33 m/s	-0.43	-0.24

5.2.1 Influence of retrofitting on 9-storey steel building

The effectiveness of the retrofitting systems on the 9-storey benchmark steel building is investigated for the chosen performance limits under the multi-hazard scenario. Fig. 7 shows the failure probability density function curves for the peak response quantities under the chosen limit states. The PDFs of the top floor acceleration and normalized base shear responses show that the mean and skewness is higher for the steel braced frame (SBF). This is attributed towards increased modal frequency, as higher stiffness attracts increased seismic force. On the other hand, for the limit states of inter-storey drift and top floor displacement, the PDFs of the MRF building has higher mean and skewness as compared to the retrofitted buildings, owing to relative flexibility. The PDFs of the peak responses for the viscoelastic damped frame (VEDF) has the least mean as compared to the PDFs of the other buildings. Therefore, it is concluded that the effects of stiffness and damping are significant in displacement response reduction under the earthquake loads. As the modal frequencies increase for the VEDF, the column base shear increases. It is observed that the VEDF has the standard deviation of the PDF closer to that of the fluid viscous damped frame (FVDF). However, the mean is lower than the mean of the FVDF. Thus, the peak displacement response is reduced due to the added damping. Under the considered wind hazard none of the limits states of failure for the responses is reached.

Fig. 8 shows the failure probabilities for the responses in terms of the cumulative distribution functions (CDFs), i.e. fragility curves under the earthquake loads. The probability of failure in the top floor acceleration is the highest in the SBF relatively. The probability of failure in the limit state of drift ratio reduces substantially on retrofitting and the lowest probability of failure is seen for the VEDF. A significant response reduction is observed due to the combined action of the added stiffness and damping in the VEDF. A significant increase in the probability of failure in the normalized base shear is observed for the SBF and VEDF, which is caused due to the increased stiffness. The probability of failure in the base shear is observed to be the least for the FVDF. The trend of the fragility curves for base shear in the SBF and VEDF is mostly similar. The additional damping decreases the failure probability in the base shear for the VEDF. The failure probability in the limit state of the top floor displacement shows a decreasing trend on retrofitting, with the VEDF having the least failure probability. Note that, the passive control devices when added to the MRF, although, reduce the failure probability, shows ineffectiveness after a certain level of the PGA. The steepness of the fragility curves for the retrofitted buildings indicates that the failure probability increases suddenly on small increase in the PGA level. Hence, the retrofitting techniques are effective at the lower PGA levels, however, may prove to be ineffective at the higher PGA levels.

5.2.2 Influence of retrofitting on 20-storey steel building

Fig. 9 shows the failure PDFs of the peak response for the top floor acceleration and inter-storey drift under the two distinct dynamic loads. The retrofitting systems for the 20-storey steel building have substantial influence on the response under the multi-hazard scenario. As observed from the PDFs of the top floor acceleration, the mean and standard deviation of the distribution has increased for the SBF as compared to the MRF. It is observed that the overlapped area of the PDFs for the SBF is lesser than that of the MRF under earthquake and wind loads. Therefore, the joint probability of failure is lower for the SBF as compared to that for the MRF.

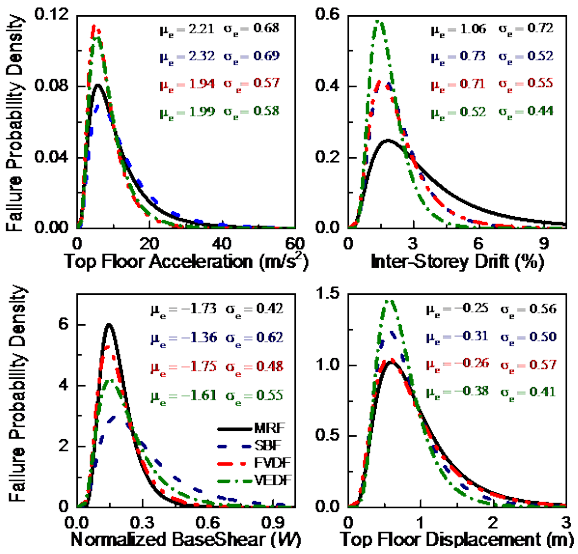

Fig. 7 - PDFs of failure for the given limit states in the 9-storey steel buildings under earthquakes

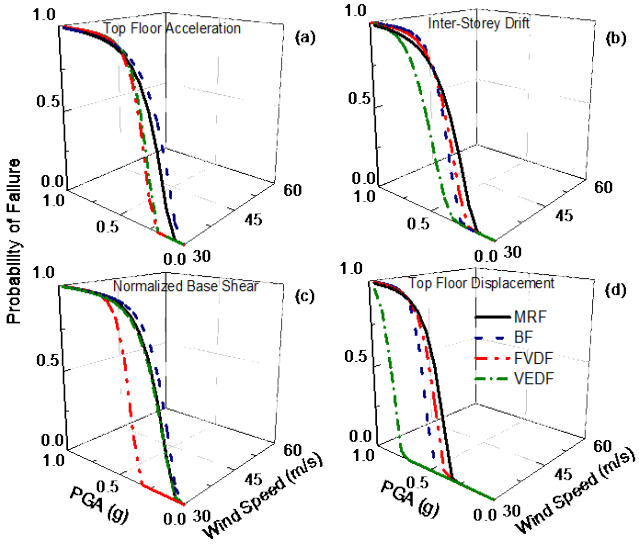

Fig. 8 - Fragility curves of the 9-storey steel buildings for the given limit states under earthquakes

The wind loads have insignificant influence on the response of the FVDF and VEDF for the top floor acceleration for the considered performance level. From the failure PDFs of the inter-storey drift, it is observed that the mean and skewness are reduced for the buildings retrofitted by the additional damping under the earthquakes and additional stiffness under the winds than the MRF. Hence, the joint probability of failure is approximately the same under both the hazards. From Fig. 10, it is observed that the mean and standard deviation of the base shear PDFs for the SBF increase substantially under the earthquake load. On the contrary, the same parameter statistics decrease substantially under the wind load. Therefore, if the buildings are retrofitted for the earthquake hazard by incorporating additional damping exhibiting substantial seismic response reduction then in case of the wind hazard similar wind response reduction is not achieved. The parameter statistics for the PDFs of the top floor displacement show that the FVDF has least mean and standard deviation as compared to that of the other steel buildings. The highest mean and standard deviation of the PDFs is observed for the SBF. Since with high stiffness favorable structural response is achieved under wind loads, no peak response reaches or exceeds the performance limits for the SBF and VEDF.

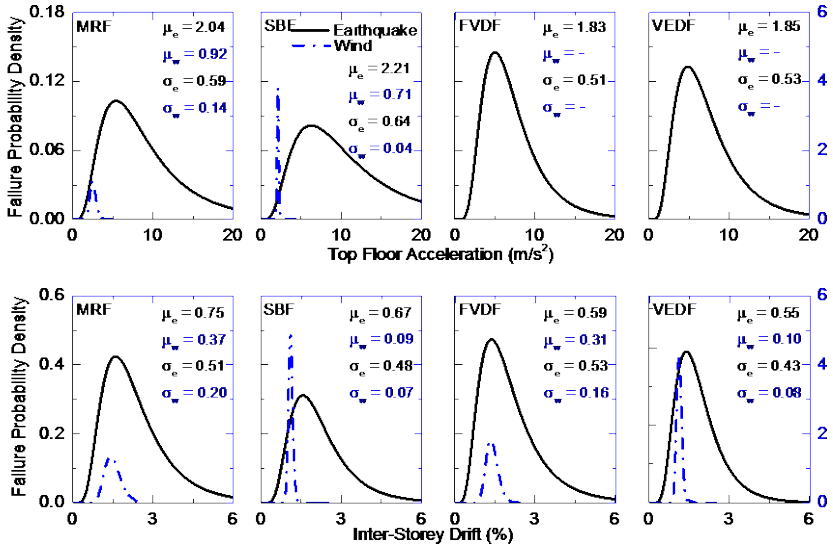

Fig. 9 - PDFs of failure in limit states of the top floor acceleration and inter-storey drift for the 20-storey steel buildings under the earthquakes and winds

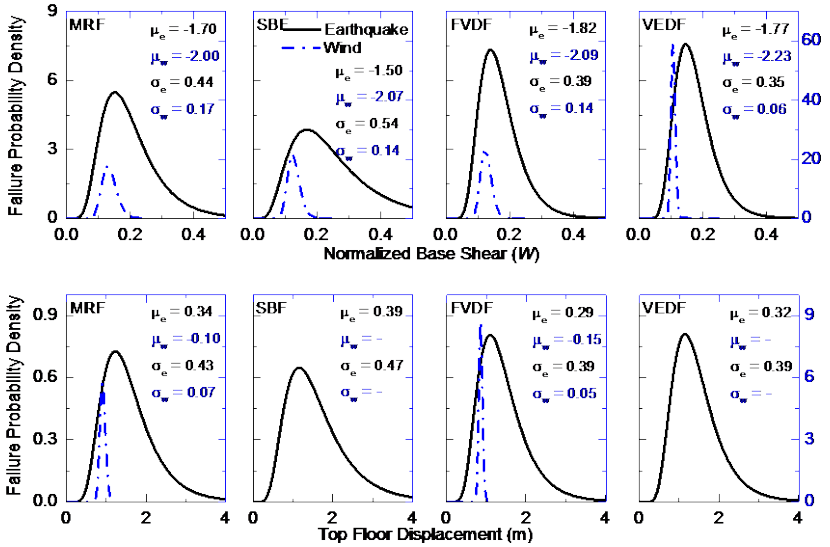

Fig. 10 - PDFs of failure in limit states of the normalized base shear and top floor displacement for the 20-storey steel buildings under the earthquakes and winds

5.2.3 Influence of retrofitting on 25-storey steel building

Figs. 11 and 12 show the PDFs of failure in different limit states for the 25-storey steel building under the earthquake and wind loads. The counteracting effects of the retrofitting are observed with increase in height of the steel buildings analyzed without and with the passive control devices. From Fig. 11, it is observed that the PDFs of the top floor acceleration for the SBF have the highest mean under earthquake load comparatively. However, the response substantially reduced on retrofitting it with the steel bracings under the wind loads. As observed earlier, the added damping helps in significant response reduction under the earthquake load and the added stiffness helps in significant response reduction under the wind loads. Hence, the joint probability of the inter-storey drift obtained for the VEDF is the least when assessed under the earthquake and wind loads. From the PDFs plotted in Fig. 12, it is observed that no peak response reach or exceed the chosen performance limits of the base shear for the earthquake hazard. The PDFs for the VEDF show a similar trend for the SBF; this calls upon careful selection of the retrofit solution and design for a structure, duly considering such multi-hazard scenario.

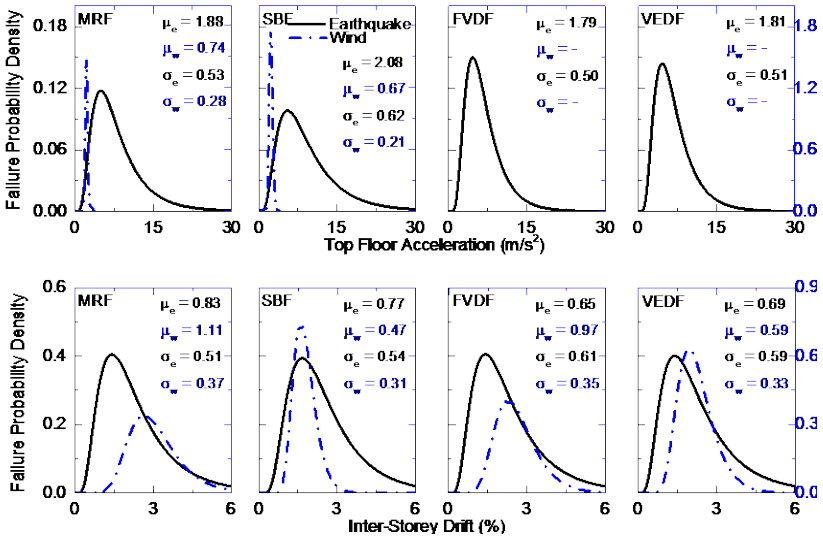

Fig. 11 - PDFs of failure in limit states of the top floor acceleration and the inter-storey drift limit states for the 25-storey steel buildings under the earthquakes and winds

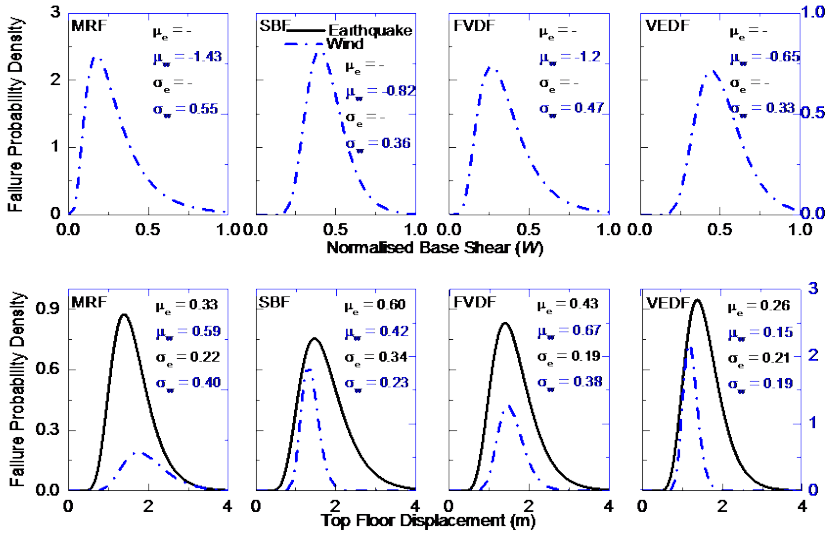

Fig. 12 - PDFs of failure in limit states of the normalized base shear and top floor displacement limit states for the 25-storey steel buildings under the earthquakes and winds

5.2.4 Seismic and wind fragility of 20- and 25-storey steel buildings

The failure probability observed in the fragility curves for the SBF is more than that of the MRF under the earthquake loads as shown in Fig. 13. The probability of failure for the FVDF is the least as compared to the failure probability of the SBF and VEDF under the earthquake loads. Similarly, it is observed that the failure probability is lower for the SBF and VEDF under the wind loads. Substantial reduction in the inter-storey drift is observed for the SBF and VEDF under the wind hazard. However, there is a steep increase in the slope of the fragility curve indicating a large increase in the failure probability with a small increase in the PGA. Moreover, for the top floor acceleration, the SBF has the least probability of failure under earthquake loads; however, the failure probability substantially increased under the wind loads. Similarly, the failure probability of the inter-storey drift is the highest for the SBF under earthquake loads, on the contrary, the least failure probability is observed under the wind loads. For the base shear, the VEDF has higher probability of failure relatively under the earthquake loads; however, the least failure probability under wind loads is observed. Hence, it is concluded that a retrofitting system which is effective in controlling the vibration response for a particular hazard; on the contrary, similar strategy may become vulnerable to the other hazard.

From the probability of failure plots shown in Fig. 14, it is observed that retrofitting by the fluid viscous damper and viscoelastic damper is effective in minimizing the seismic response efficiently for the lower PGA levels for the limit state of top floor acceleration. However, it is seen that the failure probability curves for the retrofitted buildings have steeper slopes than the failure probability curve for the MRF. This indicates the ineffectiveness of the retrofitting system, as slight increase in the PGA increases the failure probability quite largely. The failure probability for the base shear and top floor displacement shows a significant effect of the added damping to control the large deformations under the earthquake. However, the effect of additional stiffness is substantial in minimizing response under the wind hazard and is observed from the failure plot of the top floor displacement. From the inter-storey drift response, it is observed that the failure probability is the least for the FVDF under the earthquake loads; however, higher probability of failure is observed when compared with the failure probabilities in the other retrofitted buildings under the wind loads. For the top floor displacement, the SBF has the highest failure probability under the earthquake loads, however, the least failure probability is observed under the wind loads. The FVDF shows lesser probability of failure as compared to the MRF under the earthquake loads; on the contrary, it shows negligible effect against the wind loads. Therefore, it is evident from the observations that, although, a retrofit scheme is effective against a particular hazard, the vulnerability against the other hazard may increase substantially with the same retrofit scheme. Hence, a retrofit strategy providing beneficial effects against a hazard may prove to be detrimental for the other, which calls upon careful selection of the retrofit solution and design for a structure considering such multi-hazard scenario.

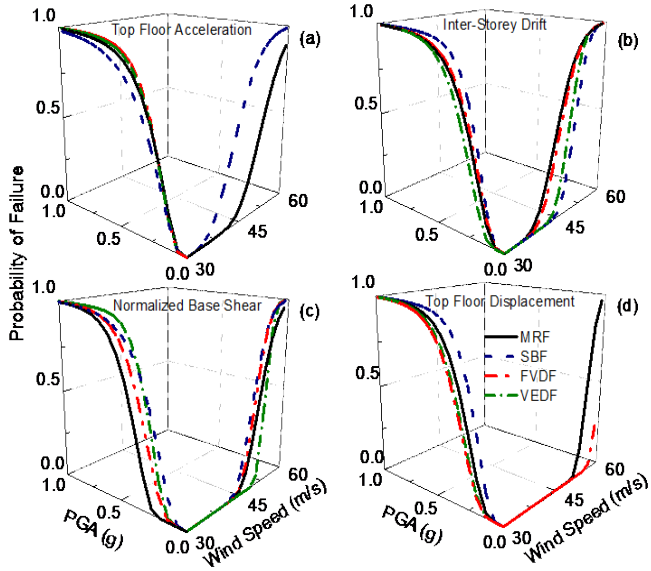

Fig. 13 - Fragility curves of the 20-storey steel buildings for given limit states under earthquakes and winds

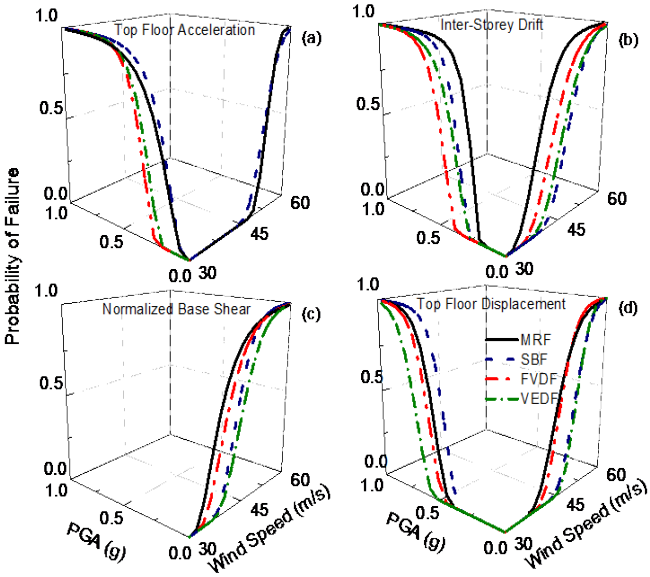

Fig. 14 - Fragility curves of the 25-storey steel buildings for given limit states under earthquakes and winds

6. Conclusions

Herein, a multi-hazard assessment of the 9-, 20-, and 25-storey steel buildings retrofitted with passive control devices, such as, steel bracing, fluid viscous damper, and viscoelastic damper is presented. The major conclusions are summarized as follows:

1. Addition of either stiffness or damping may show improved effectiveness against a particular hazard, on the contrary, it may show ineffectiveness for the other hazard. The retrofitting techniques may be effective at the lower PGA levels; however, it may prove to be ineffective at the higher PGA levels.
2. The buildings when retrofitted for the earthquake hazard by incorporating additional damping exhibiting substantial seismic response reduction, in case of the wind hazard similar wind response reduction may not be achieved essentially. Similarly, the buildings upon retrofitting by incorporation of additional stiffness indicate significant response reduction against wind loads; however, may lead to making the buildings seismic prone, i.e. increased seismic vulnerability.
3. Although, a retrofit scheme is effective against a particular hazard, the vulnerability against the other hazard may increase substantially with the same retrofit scheme. A retrofit strategy providing beneficial effects against a particular hazard may prove to be detrimental for the other, which calls upon careful selection of the retrofit solution and design for a structure considering such multi-hazard scenario.

7. References

[1] Pearce HT, Wen YK (1984): Stochastic combination of load effects. *Journal of Structural Engineering*, ASCE, **110** (7), 1613-1329.

[2] Ellingwood BR, Rosowsky DV, Li Y, Kim JH (2004): Fragility assessment of light-frame wood construction subjected to wind and earthquake hazards. *Journal of Structural Engineering*, ASCE, **130** (12), 1921-1930.

[3] Duthinh D, Simiu E (2010): Safety of structures in strong winds and earthquakes: multi-hazard considerations. *Journal of Structural Engineering*, ASCE, **136** (3), 330-333.

[4] Kameshwar S, Padgett JE (2014): Multi-hazard risk assessment of highway bridges subjected to earthquake and hurricane hazards. *Engineering Structures*, **78**, 154-166.

[5] Gehl P, D'Ayala D (2016): Development of Bayesian networks for the multi-hazard fragility assessment of bridge systems. *Structural Safety*, **60**, 37-46.

[6] Li Y, Ahuja A, Padgett JE (2012): Review of methods to assess, design for, and mitigate multiple hazards. *Journal of Performance of Constructed Facilities*, ASCE, **26** (1), 104-117.

[7] Fur LS, Yang HTY, Ankireddi S (1996): Vibration control of tall buildings under seismic and wind loads. *Journal of Structural Engineering*, ASCE, **122** (8), 948-957.

[8] Chandrasekaran S, Banerjee S (2015): Retrofit optimization for resilience enhancement of bridges under multi-hazard scenario. *Journal of Structural Engineering*, ASCE, C4015012.

[9] Ohtori Y, Christenson RE, Spencer BF, Dyke SJ (2004): Benchmark problems in seismically excited nonlinear buildings. *Journal of Engineering Mechanics*, ASCE, **130** (4), 366-385.

[10] Spencer BF, Christenson RE, Dyke SJ (1999): Next generation benchmark control problems for seismically excited buildings. *Proceedings of 2nd World Conference on Structural Control*, New York (NY), USA.

[11] Jiuhong J, Jianye D, Yu W, Hongxing H (2008): Design method for fluid viscous dampers. *Archive of Applied Mechanics*, **78** (9), 737-746.

[12] Roy T, Agarwal P (2016): Comparison of damage index and fragility curve of RC structure using different Indian standard codes. *Journal of Structural Engineering*, SERC, **43** (1), 1-9.

[13] Kwon D, Kareem A (2006): NatHaz on-line wind simulator (NOWS): simulation of Gaussian multivariate wind fields. NatHaz Modeling Laboratory Report, University of Notre Dame, Notre Dame, Indiana (IN), USA.

[14] Saha SK, Matsagar VA, Jain AK (2016): Seismic fragility of base-isolated water storage tanks under non-stationary earthquakes. *Bulletin of Earthquake Engineering*. **14** (4), 1153-1175.

[15] Dogruel S, Dargush GF (2008): A framework for multi-hazard design and retrofit of passively damped structures. Building Integration Solutions, AEI Conference, **328**, Denver, Colorado (CO), USA.